

Analyzing Bicycle Accidents with Human Body Models

Victor S. Alvarez¹, Heino Wendelrup², Karin Brolin¹

¹Lightness by Design AB, Skeppsbron 16, Stockholm, Sweden

²Hövding Sverige AB, Bergsgatan 33, Malmö, Sweden

1 Introduction

For the past 20 years, single-bicycle accidents have been the most common cycling accidents in Sweden (more than 70% of all injuries) [1-4] and in other countries where many people use bikes as means of transportation [5-6]. Vehicles were involved in a majority of the lethal bicycle accidents. Neck injuries were a small portion of all cycling injuries, but they were associated with a large risk of permanent medical impairment. Therefore, it is interesting to explore if head protective safety devices can provide safety benefits for the neck as well. Hövding is a head protective device that is worn as a scarf around the neck, with sensors that trigger inflation of an airbag in case of an accident. Theoretically, the portion of the airbag that surrounds the neck could protect from neck injuries (see Fig. 1).



Fig. 1: The physical inflated Hövding head protection device (image from www.hovding.com)

In the automotive industry, physical crash test dummies are used to assess vehicle safety. The crash test dummies are developed to be robust, provide repeatable results, and have a biofidelic response in specific loading conditions. Therefore, the ability of current crash test dummies to represent the human in bicycle accidents is strongly limited. It should be noted that none of the crash test dummies have a neck that was developed for nor can represent the complex loading situation that will occur in a bicycle accident, where the neck can be subjected to a combination of compression, shear, and bending in three dimensions. The past 20 years, finite element models of the human body have been developed with increasing anatomical details and biofidelity, in many parts of the world. Today, these human body models (HBMs) are accepted tools in automotive research and development, as objective, repeatable, and biofidelic representations of the human responses. The past ten years have seen drastic increases in research on HBM developments, and a multitude of available models exist today, including male and female representations of children, adults, and the elderly (e.g. [7-11]). HBMs with detailed models of the neck are good candidates to study neck injuries in bicycle accidents and evaluate neck protective systems.

Chalmers University of Technology has developed an HBM representing the average size female, the ViVA model [12] that is accessible in the public domain (see Fig. 2). This model was developed primarily for rear end collisions. It has an anatomically detailed neck that was validated for complex three-dimensional loading scenarios [11-13]. The Global Human Body Model Consortium has developed a range of anatomically detailed HBMs (see Fig. 3) that are available under commercial licenses (Elemance Ltd, Clemmons, North Carolina, USA. <https://www.elemance.com/>). These models have gone through a thorough and systematic development and validation (e.g. [14-16]). It is not known how well these models can represent the kinematics of a bicyclist in an accident.

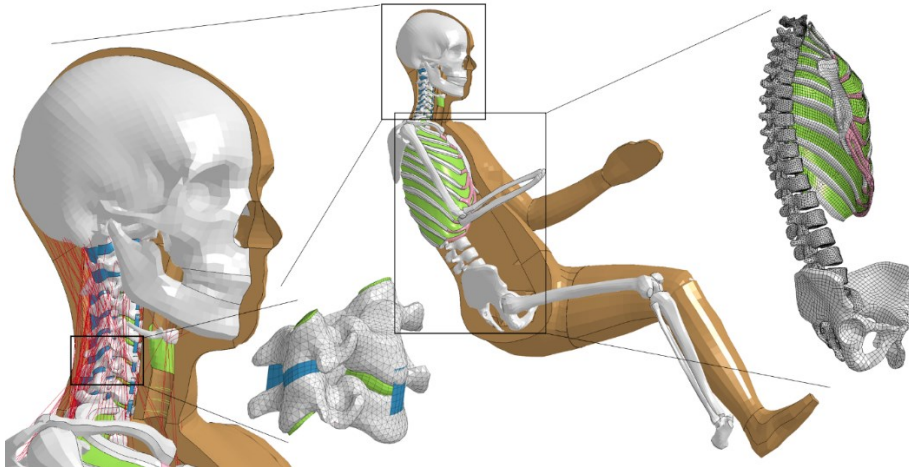


Fig.2: The ViVA model with detailed neck (www.chalmers.se/en/projects/pages/openhbm.aspx).

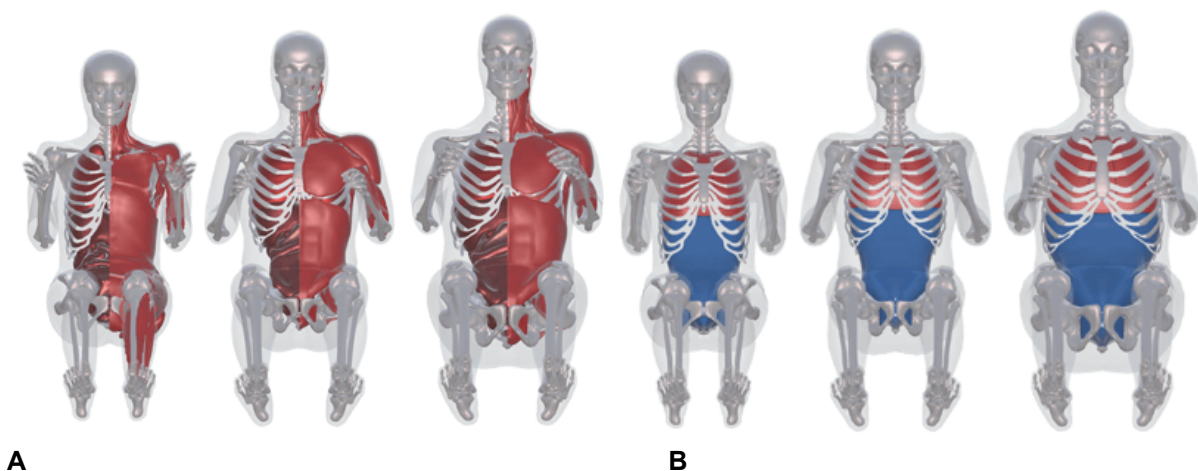


Fig.3: GHBM models representing a small female (left), average male (middle) and a large male (right) with high anatomical detail (A) and simplified (B). (<https://www.elemance.com/models/>).

The aim of this study was to evaluate the suitability of two HBMs to predict neck injuries in simulations of bicycle accidents. Therefore, this is a methodological study generating knowledge that eventually will enable systematic simulation-based neck injury risk evaluation of Hövding, and other neck protective devices, using HBMs. Included in the study were the ViVA model, representing an average sized female, and a model representing an average size male. The GHBM simplified average sized male model was chosen. The detailed model (about 2.3 million elements) requires relatively high computational resources, while the simplified model (about 840 000 elements) is about 32 times less computationally costly and easier to position.

2 Methods

The two HBM's, the ViVA average size female¹ and the GHBM simplified average male occupant model², were positioned on a finite element model of a bicycle (see Section 2.1). Due to differences in the structure of the HBMs, different methods were used to reposition them (see Sections 2.2 & 2.3). Simplified models of the Hövding airbag and a conventional cycling helmet were developed (see Sections 2.4 & 2.5). Both HBMs were compared to experimental data where a stunt person crashed into a concrete road barrier (see Section 2.6). Two head impact scenarios were simulated with both HBM's without protection, with conventional helmet and with Hövding (see Section 2.7). LS-DYNA (Ansys Inc. / LST, Canonsburg, Pennsylvania, USA) was chosen for all simulations. Neck injury criteria and thresholds were reviewed to analyze the simulation outputs.

¹ Downloaded from <https://www.chalmers.se/en/projects/pages/openhbm.aspx>

² Licensed from Elemance Ltd (Clemmons, North Carolina, USA. <https://www.elemance.com/>)

2.1 Bicycle FE model

A bicycle model developed in a previous EU project (APROSYS) [17] was used in this study. The model was a generic bicycle with deformable parts consisting of frame, handlebars, pedals, wheels, spokes and saddle (see Fig. 4). Due to the smaller anatomy of the ViVA model, the saddle and steering column were lowered 45 mm in order for the feet to reach the pedals.



Fig.4: Bicycle FE model from the EU project APROSYS study [17].

2.2 Positioning the ViVA model on the bicycle model

The ViVA model was positioned using an open-source tool developed within the EU project PIPER³. The tool uses a simplified physics-based simulation that can be run in real-time, resulting in tissue deformations as the model is positioned. This method used joints between body parts that were defined using local coordinate systems. This data was available for the ViVA model. The method did not require a separate simulation, but required some postprocessing (available in the PIPER tool) to smooth distorted elements in regions where large changes in angles were seen.

The repositioned ViVA model was then positioned above the bicycle and a simulation was done to represent the initial deformation of the buttocks and saddle. The bicycle model was translated upwards while the rigid bones in the ViVA model were constrained in all DOF. The outer soft tissue was allowed to deform. The positioned ViVA model can be seen in Fig. 5.

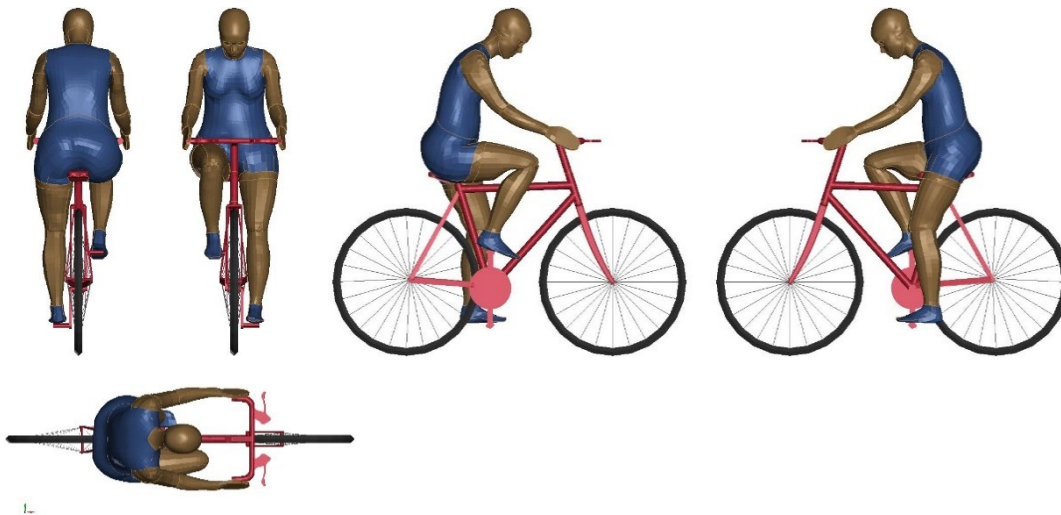


Fig.5: The ViVA model positioned on the bicycle model.

2.3 Positioning the GHBMC model on the bicycle model

The GHBMC model was positioned using a tool developed for the model. It consists of a so-called dummy-tree, which defines joints between parts that can be rotated in a preprocessor without the need of a simulation, for example using LS-PrePost. This method is often used for FE models of crash test dummies and requires local coordinate systems that can rotate relative each other. However, for HBMs, this method may result in distorted elements and a non-runnable model.

³ <http://www.piper-project.eu/start>

We used this method to define the desired position, i.e. finding the appropriate angle for knees, arms, and etcetera such that the model reaches the pedals and handle bar. In a secondary step, cables were defined between selected nodes in the original, undeformed HBM (in bony areas) and the equivalent nodal locations of the HBM in the desired position (locked in all DOF). A pretension force was applied in the cables, and a simulation was run to move the HBM into the desired position, hence avoiding the problems with severe element distortion. In this simulation, the HBM had its initial position placed a small distance above the saddle of the bicycle mode. Hence, the deformation of the buttocks and saddle was also represented during the simulation. The positioned GHBM model can be seen in Fig. 6.

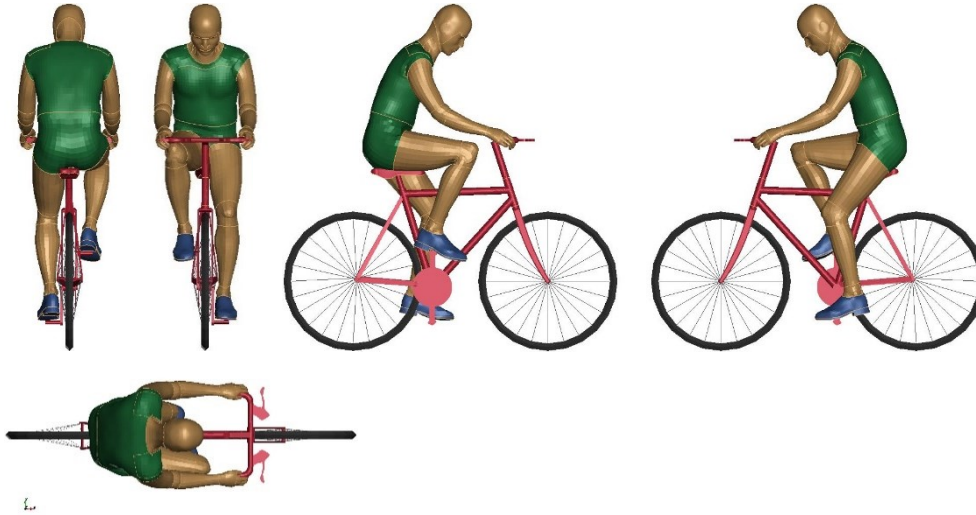


Fig. 6: The GHBM model positioned on the bicycle model.

2.4 Development of a Hövding FE Model

The physical Hövding is constructed from a planar piece of cloth with the edges forming finger like shapes. The cloth is folded and sewn together in several locations in order to achieve the final shape that can cover the head when inflated (see Fig. 1).

In this study, the geometry was simplified by only using the lower neck part of the planar drawing, that was folded in CAD to reach the closed 3D shape (see Fig. 7). A simplified version of the remaining parts of the airbag, surrounding the head, was created using half a sphere. It was then joined with the neck part by merging nodes. To mimic the shape of the inflated Hövding, the sphere part was divided into stripes that could be used to merge the nodes along the lines of the stripes. Two seams on the side of the airbag were taken from the original drawing and included in the simplified model, similarly by merging nodes. The gas-generator box was represented by a simplified geometry with similar dimensions and tied with a contact between the fabric and box. The elements included in the airbag definition were duplicated and assigned an orthotropic linear elastic material model (*MAT_FABRIC). A simple airbag model (*AIRBAG_LOAD_CURVE) was used to assign a constant pressure.

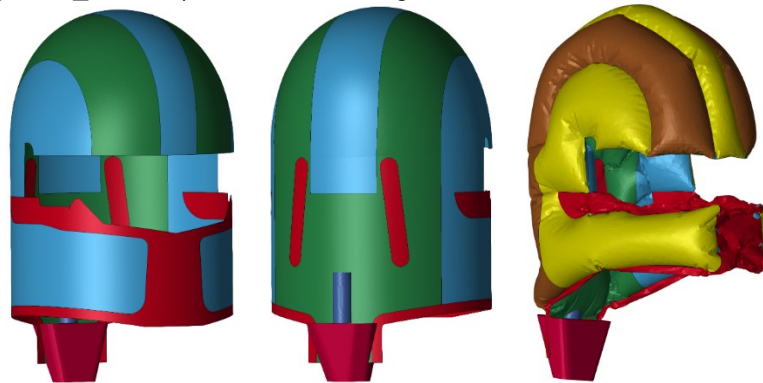


Fig. 7: Simplified Hövding FE model before inflation (two left images) and after inflation (right).

2.5 Development of a generic bicycle helmet FE model

A baseline geometry for the bicycle helmet model was downloaded from a public CAD database⁴. Then, it was adapted to fit the heads of the two HBM models and simplified, before meshing with tetrahedral elements. 25 000 solid elements and 2 550 shell elements were used to represent the foam liner material and outer shell, respectively (see Fig. 8). The material properties were taken from [18], presented in Table 1:. The outer shell was modeled with *MAT_ELASTIC and the liner with *MAT_MODIFIED_HONEYCOMB, using the load curve from [18]. The FE model was compared to a published radial impact test [18] and results are shown in Fig. 8.

Table 1: Material parameter used for helmet FE model, taken from [18].

Part	Density [kg/m ³]	Young's modulus [Gpa]	Poissons ratio [-]
Outer shell	1162	1.64	0.45
Liner	86	0.38	0.05

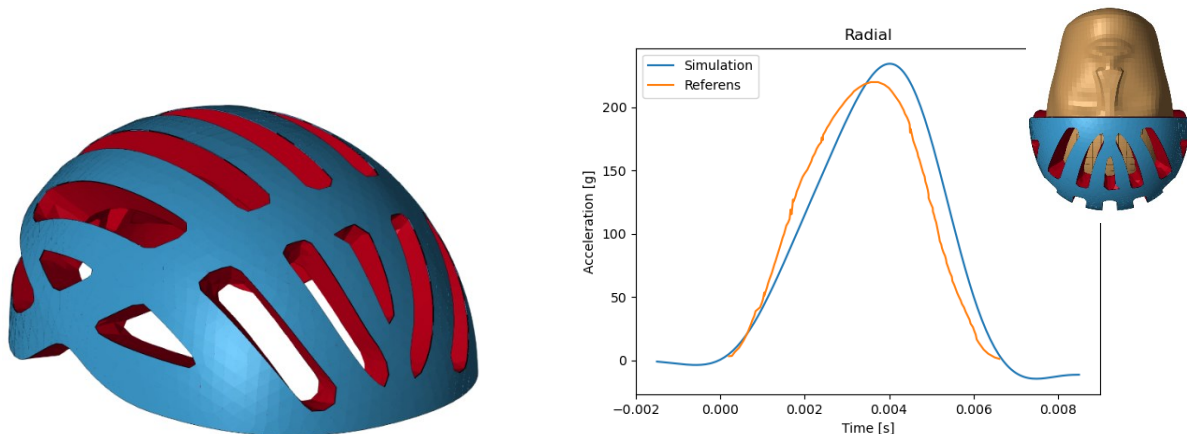


Fig.8: Helmet FE model to the left; and to the right, the comparison between simulation results with the model (blue line) and the reference test [18] (red line).

2.6 Simulation of experiment with stunt person

A representative accident scenario was chosen from experiments with stunt persons, performed internally at Hövding. It was a frontal impact in a concrete pedestrian road barrier with an initial velocity of 5 m/s (see Fig. 9). Most of the ground and a simplified concrete barrier were modeled with rigid shell elements. A small section of the ground, the predicted area for head impact, was modeled with deformable solid elements (grey square in Fig. 9). The deformable elements were given linear elastic material properties representing a midlevel coarse asphalt [19]. The concrete barrier was given a density corresponding to a weight of 250 kg. A sliding contact was defined between the ground and the barrier, with a coefficient of friction of 0.3. Constraints were defined for the hands-to-handlebar and feet-to-pedals. The constraints were active for 2 - 20 ms, in order to achieve kinematics corresponding to the video data of the experiments performed by Hövding.

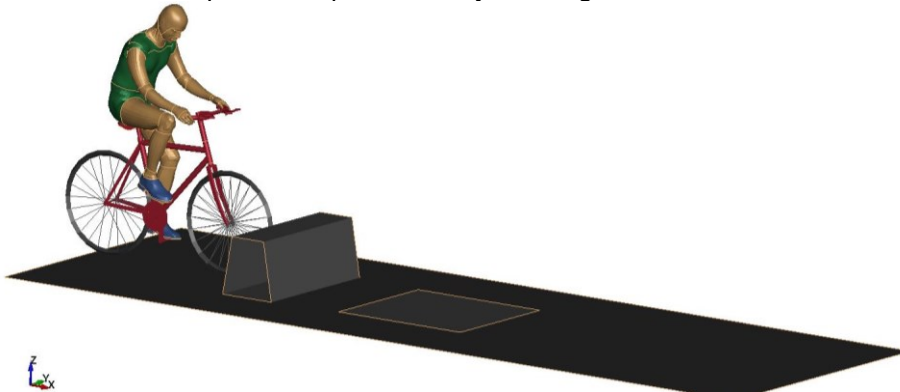


Fig.9: Simulated baseline accident scenario, frontal impact towards road suction.

⁴ <https://grabcad.com/library/bike-helmet-15>

2.7 Simulation of two head impact scenarios with three configurations of protection

Two head impact scenarios were simulated with three configurations of protection: 1) without any protective system, 2) with the simplified model of an inflated Hövding, 3) with the generic bicycle helmet model.

The first impact scenario was taken from the simulations of the stunt experiments in Section 2.6. The HBMs' positions before head impact were chosen and used to generate deformed models on which the models of Hövding and the generic bicycle helmet were positioned (see Fig. 10). For the GHBMC model, the chosen position was as close as possible to the ground impact, ensuring enough space for the Hövding airbag to inflate without ground contact. For the ViVA model, the chosen position was as close to the ground impact as possible but before neck extension increased, to facilitate realistic positioning and inflation of the Hövding airbag. The nodal velocities were also extracted at the same time step and used as initial velocities in the new simulations. An intermediate simulation was performed to inflate the simplified Hövding model, placed around the HBMs head and neck (see Fig. 11A). During this simulation the HBMs were constrained in all DOFs. In the final simulations with the Hövding, the internal pressure was activated from time zero and held constant. In the simulations with helmet, the helmet was constrained to a rigid body in the head up to a few milliseconds before ground impact.

The second impact scenario was generated by rotating the HBMs by 90 degrees about an axis corresponding to the body vertical axis (head to pelvis). This scenario was only evaluated with helmet and with Hövding (see Fig. 11B).

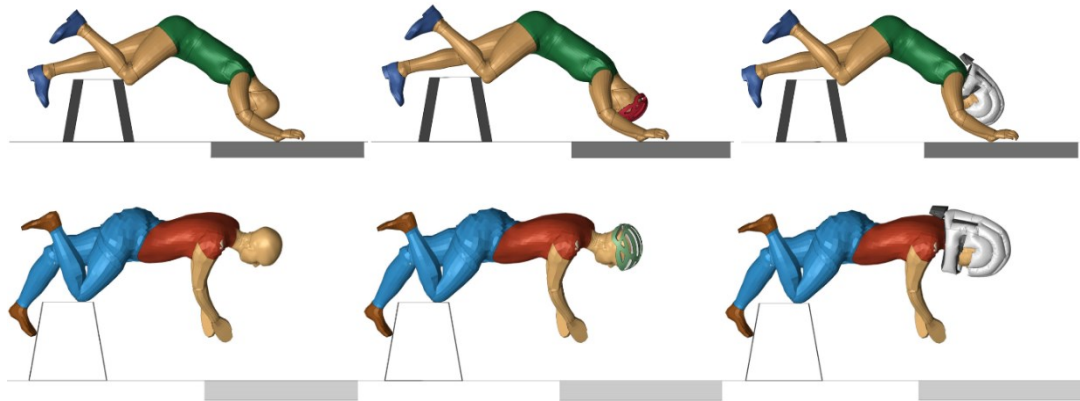


Fig.10: The two HBMs in the three configurations from left to right; no protection, with helmet and with Hövding. The GHBMC model is shown in the upper row and the ViVA model in the bottom row.

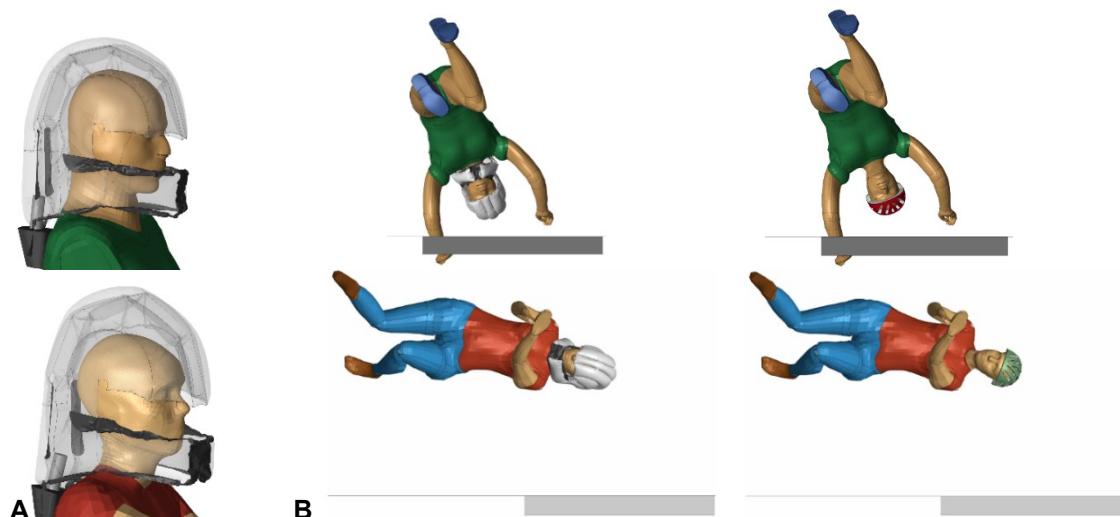


Fig.11: A. Illustration of the inflated simplified model of Hövding positioned on the HBM after the intermediate simulation. B. Second accident scenario in the two configurations; with Hövding (left) and with helmet (right). The GHBMC model (upper row) and the ViVA model (bottom row).

3 Results and discussion

3.1 Simulations compared to experiment with cycling stunt person

Fig. 13 illustrates the predicted kinematics with the GHBM and ViVA models, in the simulations of the experiment with a stunt person cycling into a concrete barrier, compared to video images. The largest differences, between the simulations and experiments, were seen for the legs and their interaction with the barrier. Both HBMs were positioned with one pedal in the lowest position and one pedal in the highest position, leading to one stretched and one bent knee. The bent knee that impacts the top of the barrier provide a pivot point that the hip rotates around, leading to a higher hip position than in the experiments. At the time of impact, the stunt person has positioned the pedals at the same level, one in the furthest forward position and one in the furthest rearward position, such that both lower legs impact the side of the barrier. Hence, the initial position of the HBM with respect to leg bending and pedal position is an important factor to capture the experimental kinematics.

The bicycle kinematics and interaction with the HBM was relatively similar to the experiments, although the modelled bike was not identical to the experimental bike. It should be noted that the sliding of the concrete barrier on the ground was important to represent the bike-barrier contact well.

The most evident difference between the GHBM and ViVA models were the neck stiffness. During the 'flight phase', the GHBMSC head did not rotate compared to the chest and the neck seem stiffer than for the stunt person. On the other hand, the ViVA model was very flexible resulting in large head extension and flexion, very different from the experiment. The difference in neck movement during flight results in very different head impact conditions for the two HBMs (see Fig. 12 & Fig. 13). The GHBM model impacts the ground with a straight neck and spine, resulting in almost pure compression, initially. The ViVA model impacts the ground with the head and neck extended, resulting in a face plant and neck loading similar to an upper cut.

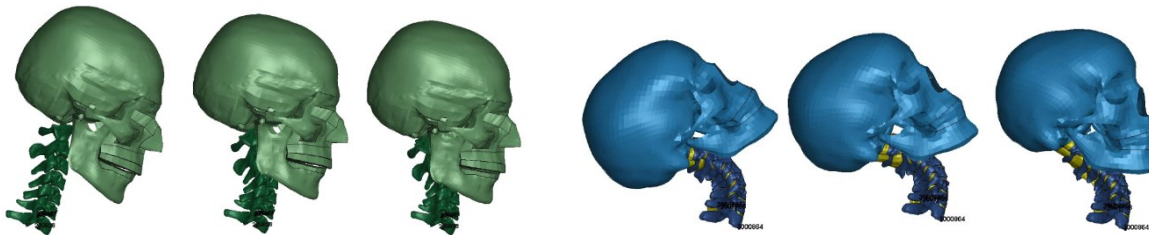


Fig.12: Illustration of head and neck kinematics just before (left) and during (middle and right) head impact to the ground. GHBM (green) and ViVA model (blue).

This comparison had several limitations, i.e.; the anthropometry of the stunt person was not matched by the HBMs, the bike model was not validated to the bike model in the experiment, the stunt person expects an impact and braces accordingly and prepares for landing right before head impact, only one stunt experiment and one impact was included. It is a first promising indication that both HBMs can capture the kinematics in cycling accidents. It highlighted the importance of initial pedal positions, the feasibility of using tied contacts for hand-handlebar and feet-pedals released based on video analyses of the experiments, and the differences in neck stiffness between the two HBMs. The ViVA model was numerically unstable and required manual hands-on adjustments of facet joint contacts and the mesh of soft tissues and to avoid error termination due too negative volume in solid elements. The low stiffness of soft tissue representing flesh and skin was the main contributing factor to instability, however we did not change any material properties. It seems likely that the ViVA model is too weak for this load scenarios and needs improvement of robustness. This work is ongoing in the VIRTUAL project⁵, and we look forward to evaluate the improved version of the average female model when validations have been completed.

⁵ <https://projectvirtual.eu/>

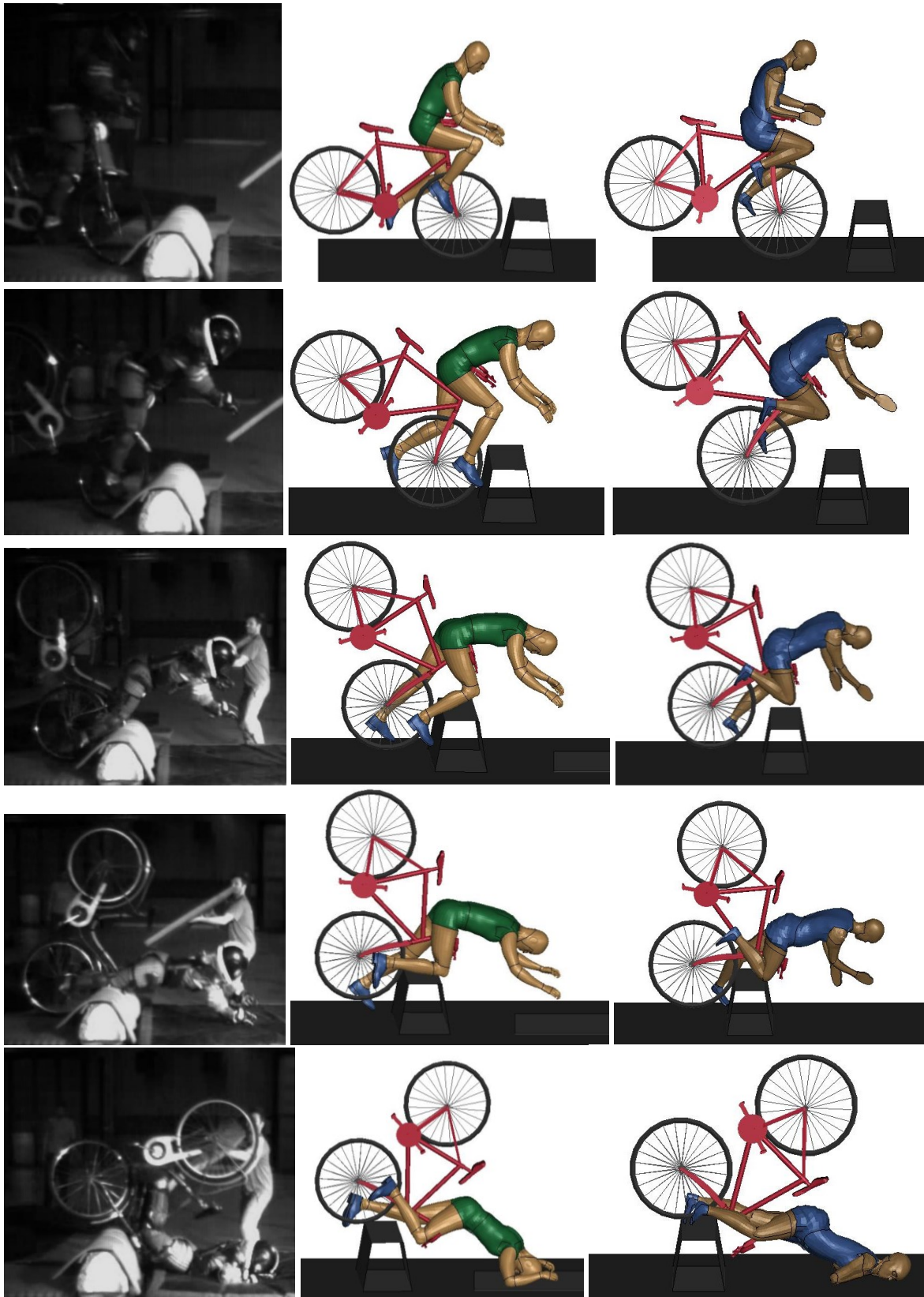


Fig.13: Comparison of experimental test with stunt person cycling into a concrete barrier (left) and the corresponding simulations with the GHMBC model (middle) and ViVA model (right).

3.2 Evaluation of neck injuries

There are global injury criteria, often used together with crash test dummies, and tissue level criteria, often used with anatomically detailed HBMs, see Table 2 for a summary. Tissue level criteria are for example the strains in the ligaments (to predict soft tissue injury) or stress in the vertebrae (to predict fracture). Global injury criteria use accelerations, forces and moments from crash test dummy measurements and are compared with experimental test thresholds. The simplified GHMBC has joints between the vertebrae. The forces and moments in these joints can be post-processed to represent the dummy reading, which requires transformation of the simulation output to a location equivalent to the sensor location in the mechanical dummy. For some of the global criteria in Table 2, this script was readily available from Elemance Ltd, which we then needed to further develop in order to get output for the remaining global injury criteria. The ViVA model has an anatomically detailed neck with deformable vertebrae, ligaments and intervertebral discs. It is therefore well suited to use tissue level criteria. On the other hand, global injury criteria would require minor model modifications to measure forces and moments.

Table 2: Summary of neck injury criteria that can be used with the two HBMs. * Requires additional scripts. ** Requires minor model modifications to get output.

Injury criteria	References	GHMBC M50-OS	ViVA F50
NIC	[20-21]	Yes	Yes
Nkm	[22]	Yes	Yes **
Nij	[23-24]	Yes	Yes **
S-shape of neck	e.g. [25-28]	Yes*	Yes, visual inspection.
Extension moment	[29]	Yes	Yes **
Flexion moment	[29-30]	Yes	Yes **
Compressile force	[31]	Yes	Yes **
Tensile force	[29-31]	Yes	Yes **
Shear force	[31-32]	Yes	Yes **
Stress in vertebral bone	[33]	No	Yes
Ligament tension	[34-35]	No	Yes
Vertebral dislocations		No	Yes, visual inspection.

3.3 Simulation of two head impact scenarios with three configurations of protection

All head impact simulations ran without numerical issues for all three configurations: 1) without any protective system, 2) with the simplified model of an inflated Hövding, 3) with the generic bicycle helmet model.

Table 3 lists the resulting output for relevant injury criteria in the simulations with the GHMBC model. Head injury is predicted without protection, while both the helmet and Hövding model reduces the head injury criteria (HIC) well below the threshold. GHMBC predicts compressive injury in all simulations and low bending moments well below the thresholds. This is likely a direct effect of the straight spine in the impact, and it should be further explored if the neck stiffness of the simplified GHMBC is too stiff for these loading conditions. Fig. 14 presents ligament strains and vertebral stress for the simulations with the ViVA model. No clear trend can be seen and the difference are too small to make any conclusions on protective capacity.

It was clear from a visual inspection of the simulations that the simplified model of the Hövding moved superiorly during the inflation process, such that the collar portion och airbag moved from a location around the neck to the chin (see Fig. 15). This phenomenon does not occur with the physical Hövding, and therefore indicates that an improved model is required. An improved model needs to model the whole Hövding in detail and be validated regarding internal pressure of the different parts during inflation as well as for dynamic head impact responses, if possible, with a physical drop test using crash test dummy components.

Table 3: Results for relevant head and neck injury criteria with the GHMBC model in the two head impact scenarios.

		Scenario 1			Scenario 2		Threshold
		Without protection	Helmet	Hövding	Helmet	Hövding	
HIC		5523	760	415	565	88	1000
Nij		0.43	0.38	0.39	0.41	0.26	1
Nkm		1.97	1.87	1.71	2.95	2.63	1
Extension moment	Nm	9	8	8	10	10	75
Flexion moment	Nm	23	23	23	20	9	190
Lateral moment	Nm	24	21	13	24	18	lacking
Compression	kN	-2.6	-2.0	-2.0	-2.2	-1.5	1.1 - 4.0
Tension	kN	0.2	0.3	0.3	0.2	0.2	1.1 - 3.1
Shear	kN	1.3	1.2	1.0	2.2	2.1	1.1 - 3.1

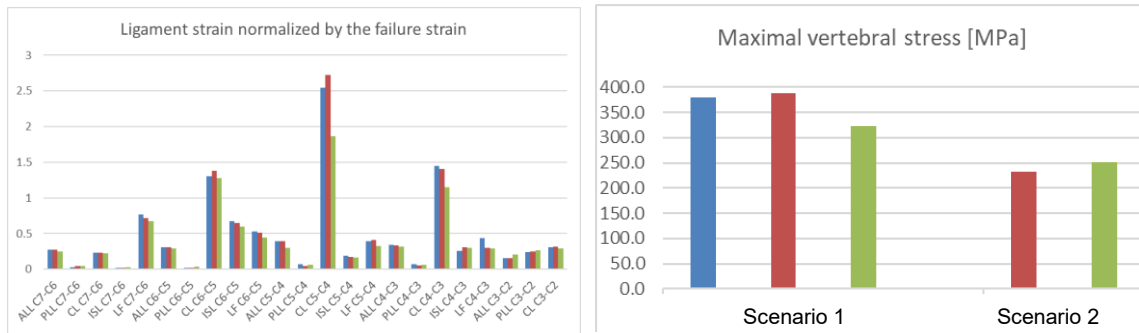


Fig. 14: Resulting ligament strain (left) and vertebral stress (right) for the ViVA model without protection (blue bars), with the generic helmet (red bars), and with the inflated simplified Hövding (green bars).

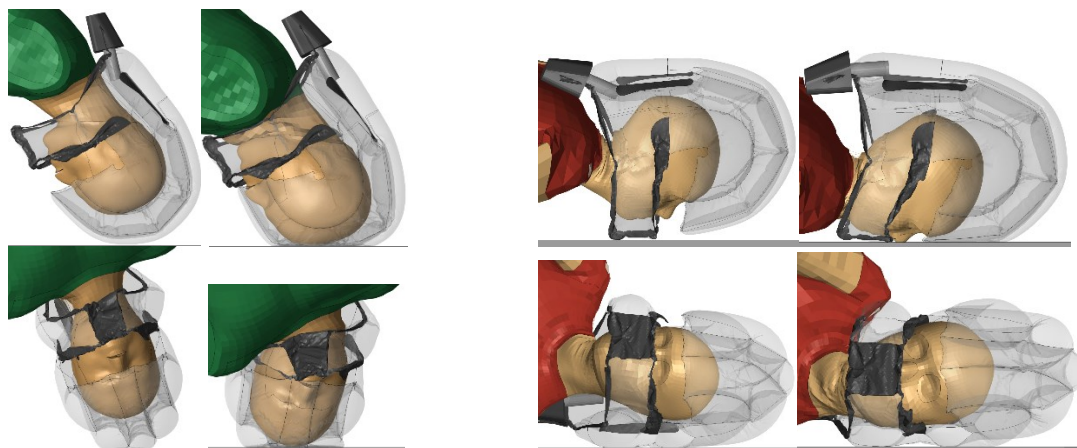


Fig. 15: GHMBC (green) and ViVA model (red) with the inflated simplified model of Hövding at the time of ground contact (left) and during the impact (right), for scenario 1 (top) and scenario 2 (bottom).

4 Summary

The GHBM average size male simplified occupant model and the ViVA average size female occupant model used to simulate an experimental bicycle crash scenario and two head impacts with three protective configurations. Our results indicate that the methodology is promising. The ViVA model had issues with numerical instability due to low stiffness of soft tissues and required manual improvement to run through the whole accident scenario. The simplified GHBM model was numerically robust but seemed a bit stiff, which needs to be studied further. Both HBMs could be combined with relevant neck injury criteria, either global dummy type criteria or tissue level criteria. Its main conclusions were that: 1) the initial position of the legs and feet on the pedals were important for the accident kinematics, 2) the concrete road barrier friction and sliding on the ground was important to capture a realistic bike-barrier response, 3) more experimental data representing other accident scenarios need to be simulated and compared to, and 4) the simplified model of Hövding was too limited to draw any conclusions regarding reduction of neck injuries and an improved model that is validated will be needed to do that. Although its limitations, this study shows that the used methodology is promising and indicates that the selected HBMs may provide valuable tools for assessment of cycling safety systems.

5 Acknowledgement

This study was funded by Skyltfonden⁶ (Trafikverket, Sweden), all conclusions are those of the authors and not necessarily agreed upon by the funding agency. The authors acknowledge Autoliv Research AB for providing the bicycle model.

6 Literature

- [1] Kjeldgård L, Ohlin M, Elreud R, et al. (2019) Bicycle crashes and sickness absence - a population-based Swedish register study of all individuals of working ages. BMC Public Health 19:943. <https://doi.org/10.1186/s12889-019-7284-1>
- [2] Trafikverket (2014). Safer cycling – a common strategy for the period 2014–2020, Version 1.0. Trafikverket, rapport 2014:35. <https://trafikverket.ineko.se/se/tv17634>
- [3] Niska A, and Eriksson J (2013). Cycling accident statistics. Background information to the common policy strategy for safe cycling. VTI report 801. ISSN 0347-6030. <https://www.diva-portal.org/smash/get/diva2:694821/FULLTEXT01.pdf> [in Swedish, English abstract only]
- [4] Rizzi M, Stigson H, Krafft M. (2013) Cyclist Injuries Leading to Permanent Medical Impairment in Sweden and the Effect of Bicycle Helmets. Proceedings of IRCOBI Conference, Gothenburg, Sweden. IRC-13-46. http://www.ircobi.org/wordpress/downloads/irc13/pdf_files/46.pdf
- [5] Amoros, E., Chiron, M., Martin, J.L., Thélot, B., Laumon, B., 2012. Bicycle helmet wearing and the risk of head, face, and neck injury: A French case-control study based on a road trauma registry. Inj. Prev. 18, 27–32. <http://dx.doi.org/10.1136/ip.2011.031815>
- [6] Schepers P, Klein Wolt K (2012) Single-bicycle types and characteristics. Cycling Research International, 2:119 – 135
- [7] Jones DA, Gaewsky JP, Somers JT et al. (2020). Head injury metric response in finite element ATDs and a human body model in multidirectional loading regimes. Traffic Inj Prev. 2019;20(sup2):S96-S102. <https://doi.org/10.1080/15389588.2019.1707193>
- [8] Hu J, Zhang K, Reed M, et al. (2018) Frontal crash simulations using parametric human models representing a diverse population. Traffic Injury Prevention 20: S97-S105. <https://doi.org/10.1080/15389588.2019.1581926>
- [10] Iraeus J, Brolin K, Pipkorn B. (2020) Generic finite element models of human ribs, developed and validated for stiffness and strain prediction - To be used in rib fracture risk evaluation for the human population in vehicle crashes. Journal of the Mechanical Behavior of Biomedical Materials, 106. <http://dx.doi.org/10.1016/j.jmbbm.2020.103742>
- [11] Östh J, Mendoza-Vazquez M, Sato F, et al. (2017). A female head–neck model for rear impact simulations. Journal of Biomechanics 51:49-56. <https://doi.org/10.1016/j.jbiomech.2016.11.066>
- [12] Östh J, Mendoza-Vazquez M, Linder A, et al. (2017) The ViVA OpenHBM Finite Element 50th Percentile Female Occupant Model: Whole Body Model Development and Kinematic Validation. Proceedings of IRCOBI Conference, Antwerp, IRC-17-60. <http://www.ircobi.org/wordpress/downloads/irc17/pdf-files/60.pdf>
- [13] Östh J, Brolin L, Svensson MY, and Linder A (2016) A Female Ligamentous Cervical Spine Finite Element Model Validated for Physiological Loads. J. Biomech. Eng. 138(6):061005. <https://doi.org/10.1115/1.4032966>
- [14] Barker JB, Cronin D. (2020) Multi-level Validation of a Male Neck Finite Element Model with Active Musculature. J Biomech Eng. 143(1):011004. <https://doi.org/10.1115/1.4047866>
- [15] Cronin, D. S., Fice, J., DeWit, J. et al. (2012) Upper cervical spine kinematic response and injury prediction. in Proceedings of IRCOBI Conference, Dublin, Ireland. IRC-12-30. http://www.ircobi.org/wordpress/downloads/irc12/pdf_files/30.pdf
- [16] Lasswell TL, Cronin DS, Medley JB et al. (2017). Incorporating ligament laxity in a finite element model for the upper cervical spine. Spine J. 17(11):1755-1764. <https://doi.org/10.1016/j.spinee.2017.06.040>

⁶ <https://www.trafikverket.se/om-oss/var-verksamhet/sa-har-jobbar-vi-med/Vart-trafiksakerhetsarbete/Skyltfonden/>

- [17] Hardy RN, et al. (2004). Impact conditions for pedestrians and cyclists - APROSYS Deliverable D3.2.3. p.43-44. https://trimis.ec.europa.eu/sites/default/files/project/documents/20120313_143640_26037_AP-SP32-009R_D323.pdf
- [18] Fahlstedt M, Halldin P, and Kleiven S, (2016). The Protective Effect of a Helmet in Three Bicycle Accidents - A Finite Element Study. *Accid. Anal. Prev.* 91:135–143. <https://doi.org/10.1016/j.aap.2016.02.025>
- [19] Setiawan A, Suparna LB, and Mulyono AT (2017). Developing the elastic modulus measurement of asphalt concrete using the compressive strength test. *AIP Conference Proceedings* 1903: 050002. <https://doi.org/10.1063/1.5011541>
- [20] Boström O, Svensson M, Aldman B, et al. (1996) A new neck injury criterion candidate based on injury findings in the cervical spinal ganglia after experimental neck extension trauma. *Proceedings of IRCOBI Conference, Dublin, Ireland.* http://www.ircobi.org/wordpress/downloads/irc1996/pdf_files/1996_9.pdf.
- [21] Bohmann K, Boström O, Håland Y, Kullgren A (2000) A study of AIS1 neck injury parameters in 168 frontal collisions using a restraint Hybrid III dummy. *Proceedings of 44th Stapp Car Crash Conference*, pp 103–116
- [22] Schmitt K-U, Muser M, Walz F, Niederer P (2002a) Nkm—a proposal for a neck protection criterion for low speed rear-end impacts. *Traffic Injury Prevention* 3(2):117–126. <https://doi.org/10.1080/15389580212002>
- [23] Kleinberger M, Sun E, Eppinger R, Kuppa S, Saul R (1998) Development of improved injury criteria for the assessment of advanced automotive restraint systems. NHTSA report, September 1998.
- [24] Duma S, Crandell J, Rudd R, Funk J, Pilkey W (1999) Small female head and neck interaction with a deploying side air bag. *Proceedings of IRCOBI Conference, Sitges, Spain.* http://www.ircobi.org/wordpress/downloads/irc1999/pdf_files/1999_14.pdf
- [25] Ono K, Kaneoka K (1997) Motion analysis of human cervical vertebrae during low speed rear impacts by the simulated sled. *Proceedings of IRCOBI Conference, Hanover, Germany.* http://www.ircobi.org/wordpress/downloads/irc1997/pdf_files/1997_14.pdf
- [26] Ono K, Kaneoka K, Imami S (1998) Influence of seat properties on human vertebral motion and head/neck/torso kinematics during rear end impacts. *Proceedings of IRCOBI Conference, Gothenburg, Sweden.* http://www.ircobi.org/wordpress/downloads/irc1998/pdf_files/1998_22.pdf
- [27] Grauer J, Panjabi M, Cholewicki J, Nibu K, Dvorak J (1997) Whiplash produces an S-shaped curvature on the neck with hyperextension at lower level. *Spine* 22(21):2489–2494
- [28] Svensson M, Aldman B, Hansson H, et al. (1993) Pressure effects in the spinal canal during whiplash extension motion: a possible cause of injury to the cervical spine ganglia. *Proceedings of IRCOBI Conference, Eindhoven, The Netherlands.* http://www.ircobi.org/wordpress/downloads/irc1993/pdf_files/1993_13.pdf
- [29] Goldsmith W, Ommaya AK (1984) Head and neck injury criteria and tolerance levels. In: Aldman B, Chapon A (eds) *The biomechanics of impact trauma.* Elsevier Science Publishers, Amsterdam, pp 149–187
- [30] Mertz H, Patrick L (1971) Strength and response of the human neck. *Proceedings of 15th Stapp Car Crash Conference, SAE 710855*, pp 207–255
- [31] Myers B, McElhaney J, Richardson W, Nightingale R, Doherty B (1991) The influence of end conditions on human cervical spine injury mechanisms. *Proceedings of 35th Stapp Car Crash Conference SAE 912915*, pp 391–400
- [32] Doherty B, Esses S, Heggeness M (1993) A biomechanical study of odontoid fractures and fracture fixation. *Spine* 18(2):178–184. <https://doi.org/10.1097/00007632-199302000-00002>
- [33] Halldin P, Brolin K, Kleiven S, Jakobsson L, Palmertz C, and von Holst H. (2000) Investigation of Conditions that Affect Neck Compression-Flexion Injuries Using Numerical Techniques. *Proceedings of 44th Stapp Car Crash Conference, 2000-01-SC10.*
- [34] Yoganandan N, Kumaresan S, and Pintar F. (2001) Biomechanics of the cervical spine. Part 2: Cervical spine soft tissue responses and biomechanical modelling, *Clin. Biomech.* 16(1):1–27. [https://doi.org/10.1016/S0268-0033\(00\)00074-7](https://doi.org/10.1016/S0268-0033(00)00074-7)
- [35] Myklebust JB, Pintar F, Yoganandan N, et al. (1988) Tensile strength of spinal ligaments. *Spine* 13(5):526–531.